



Research article

Piecewise differential equations: theory, methods and applications

Abdon Atangana^{1,2,*} and Seda İğret Araz^{1,3}

¹ Faculty of Natural and Agricultural Sciences, University of the Free State, South Africa

² Department of Medical Research, China Medical University Hospital, China Medical University, Taichung, Taiwan

³ Faculty of Education, Siirt University, Siirt 56100, Turkey

* **Correspondence:** Email: AtanganaA@ufs.ac.za.

Abstract: Across many real-world problems, crossover tendencies are seen. Piecewise differential operators are constructed by using different kernels that exhibit behaviors arising in several real-world problems; thus, crossover behaviors could be well modeled using these differential and integral operators. Power-law processes, fading memory processes and processes that mimic the generalized Mittag-Leffler function are a few examples. However, the use of piecewise differential and integral operators cannot be applied to all processes involving crossovers. For instance, a considerable alteration eventually manifests when groundwater over-abstraction causes it to flow from confined to unconfined aquifers. The idea of piecewise differential equations, which can be thought of as an extension of piecewise functions to the framework of differential equations, is introduced in this work. While we concentrate on ordinary differential equations, it is important to note that partial differential equations can also be constructed with the same technique. For both integer and non-integer instances, piecewise differential equations have been introduced. We have explained the usage of the Laplace transform for the linear case and demonstrated how a new class of Bode diagrams could be produced. We have provided some examples of numerical solutions as well as conditions for the existence and uniqueness of their solutions. We discussed a few scenarios in which we used chaos and non-linear ordinary differential equations to produce novel varieties of chaos. We believe that this idea could lead to some significant conclusions in the future.

Keywords: piecewise differential equations; Laplace transform; Bode diagram; numerical scheme; new chaotic attractors

Mathematics Subject Classification: 34K28, 37D45, 44A10

1. Introduction

Chaotic behaviors can be seen throughout nature, and some of them have recently been replicated using mathematical models. Existing models, in particular chaotic processes with crossover characteristics, nevertheless fail to account for some phenomena. When the idea of piecewise differentiation and integration was first presented, this category of chaotic processes received very little attention [1]. With this idea, a differential operator in a chaotic model is changed by replacing it with a piecewise derivative that entails defining an alternative differential operator in an interval. The use of this idea has, in fact, opened up more research directions toward a revolution in the study of chaos, and new chaotic attractors have been found. However, in this instance, the only thing that changes is differentiation. Thus, crossovers are caused by the characteristics of the kernels utilized, which can be the power-law [2], generalized Mittag-Leffler [3], exponential decay function [4] or the Dirac delta function. A novel concept is required because some crossover phenomena cannot be described using piecewise differential operators. As an example, nowadays people can envisage worlds that may exist but are not present in their daily lives thanks to the cinema industry; for instance, a horse with a human head, people with long tails, like in the movie *Avatar*, and several other examples that can be listed. Perhaps the core sciences could benefit from using this creativity to combine two concepts into one new thought. This idea could be used to address a particular procedure in the actual world. To address a particular real-world process that could not be recreated using current theories, such a concept might be put forth. This ought to apply to the study of mathematics and its applications [5–19]. For instance, one may consider a high level of crossover that could consist of describing the chaos processes at various intervals to capture crossings that cannot be replicated using piecewise differential operators. Piecewise differential equations will be used to refer to this idea where the processes governing the function fluctuate with time. This idea can be seen as a piecewise function application, which has various uses in simulating human behavior and other real-world problems. Piecewise functions have only been utilized in differential equations to change parameters and source procedures. Although there are references to these processes in the literature, an overarching theory has yet to be created. The problem of the movement of groundwater provides a vivid illustration. This problem has been described as a piecewise differential equation system, where the first portion takes into account flow in a confined aquifer, and the second part takes into account flow in an open aquifer. It is important to note that this approach differs greatly from the notion of an equation system in which all of the variables behave within the same time interval and with the same sub-governing functions. In this paper, we look into several practical uses for this family of differential equations.

2. Definition of Cauchy piecewise problem

In this section, we present some cases of the piecewise Cauchy problems where different piecewise derivatives are used.

Case 1: Classical Cauchy piecewise problem

Let f_1, f_2, \dots, f_n be linear or non-linear, bounded and continuous functions. A piecewise ordinary differential equation is defined as

$$\frac{d}{dt}u(t) = \begin{cases} f_1(t, u(t)) & \text{if } 0 \leq t \leq t_1 \\ f_2(t, u(t)) & \text{if } t_1 \leq t \leq t_2 \\ \vdots & \\ f_n(t, u(t)) & \text{if } t_{k-1} \leq t \leq t_k \end{cases} . \quad (2.1)$$

Case 2: Cauchy piecewise problem with power-law

Let f_1, f_2, \dots, f_n be linear or non-linear bounded and continuous functions; let the function $u(t)$ be differentiable. A piecewise problem with the power-law [2] is represented by

$${}_0^C D_t^\alpha u(t) = \begin{cases} f_1(t, u(t)) & \text{if } 0 \leq t \leq t_1 \\ f_2(t, u(t)) & \text{if } t_1 \leq t \leq t_2 \\ \vdots & \\ f_n(t, u(t)) & \text{if } t_{k-1} \leq t \leq t_k \end{cases} . \quad (2.2)$$

Case 3: Cauchy piecewise problem with Mittag-Leffler

Let f_1, f_2, \dots, f_n be linear or non-linear bounded and continuous functions; let the function $u(t)$ be differentiable. A piecewise problem with the Mittag-Leffler function [3] is defined by

$${}_0^{ABC} D_t^\alpha u(t) = \begin{cases} f_1(t, u(t)) & \text{if } 0 \leq t \leq t_1 \\ f_2(t, u(t)) & \text{if } t_1 \leq t \leq t_2 \\ \vdots & \\ f_n(t, u(t)) & \text{if } t_{k-1} \leq t \leq t_k \end{cases} . \quad (2.3)$$

Case 4: Cauchy piecewise problem with exponential decay

Let f_1, f_2, \dots, f_n be linear or non-linear bounded and continuous functions; let the function $u(t)$ be differentiable. A piecewise problem with exponential decay [4] can be written as

$${}_0^{CF} D_t^\alpha u(t) = \begin{cases} f_1(t, u(t)) & \text{if } 0 \leq t \leq t_1 \\ f_2(t, u(t)) & \text{if } t_1 \leq t \leq t_2 \\ \vdots & \\ f_n(t, u(t)) & \text{if } t_{k-1} \leq t \leq t_k \end{cases} . \quad (2.4)$$

Remark. More generally, the following piecewise differential system can be written as

$$\left\{ \begin{array}{l} u'(t) = \begin{cases} f_1(t, u(t)) & \text{if } 0 \leq t \leq t_1 \\ f_2(t, u(t)) & \text{if } t_1 \leq t \leq t_2 \\ \vdots \\ f_{n_1}(t, u(t)) & \text{if } t_{k-1} \leq t \leq t_k \end{cases}, \text{ if } 0 \leq t \leq \tilde{t}_1 \\ {}^{CF}_{\tilde{t}_1} D_t^\alpha u(t) = \begin{cases} f_1(t, u(t)) & \text{if } 0 \leq t \leq t_1 \\ f_2(t, u(t)) & \text{if } t_1 \leq t \leq t_2 \\ \vdots \\ f_{n_2}(t, u(t)) & \text{if } t_{k-1} \leq t \leq t_k \end{cases}, \text{ if } \tilde{t}_1 \leq t \leq \tilde{t}_2 \\ \vdots \\ {}^{ABC}_{\tilde{t}_{k-1}} D_t^\alpha u(t) = \begin{cases} f_1(t, u(t)) & \text{if } 0 \leq t \leq t_1 \\ f_2(t, u(t)) & \text{if } t_1 \leq t \leq t_2 \\ \vdots \\ f_{n_l}(t, u(t)) & \text{if } t_{k-1} \leq t \leq t_k \end{cases}, \text{ if } \tilde{t}_{k-1} \leq t \leq \tilde{t}_k \end{array} \right. \quad (2.5)$$

3. Laplace transform with examples

When the functions f_i are linear, the solution can be derived by using the Laplace transform. We give an example of course using the same technique for a piecewise function. We shall present the Laplace transform of Example 1; indeed, the rest can be done similarly.

$$\begin{aligned} \frac{d}{dt}u(t) &= (u(t) - u(t - t_1)) f_1(t, u(t)) \\ &\quad + (u(t - t_2) - u(t - t_3)) f_2(t, u(t)) \\ &\quad + \dots + u(t - t_n) f_n(t, u(t)). \end{aligned} \quad (3.1)$$

We can apply the Laplace transform on both sides to obtain

$$\tilde{s}u(s) - u(0) = \sum_{j=1}^n \left[\begin{array}{l} e^{-st_j} L(f_j(t + t_j, u(t + t_j))) \\ -e^{-st_{j-1}} L(f_{j-1}(t + t_{j-1}, u(t + t_{j-1}))) \end{array} \right]. \quad (3.2)$$

Our next challenge is to find $L(f_j(t + t_j, u(t + t_j)))$.

In the case of the power-law, we have

$$s^\alpha \tilde{u}(s) - s^{\alpha-1} u(0) = \sum_{j=1}^n \left[\begin{array}{l} e^{-st_j} L(f_j(t + t_j, u(t + t_j))) \\ -e^{-st_{j-1}} L(f_{j-1}(t + t_{j-1}, u(t + t_{j-1}))) \end{array} \right]. \quad (3.3)$$

In the case of the Mittag-Leffler function, we have

$$\frac{1}{1-\alpha} \frac{s^\alpha \tilde{u}(s) - s^{\alpha-1} u(0)}{s^\alpha + \frac{\alpha}{1-\alpha}} = \sum_{j=1}^n \left[\begin{array}{l} e^{-st_j} L(f_j(t + t_j, u(t + t_j))) \\ -e^{-st_{j-1}} L(f_{j-1}(t + t_{j-1}, u(t + t_{j-1}))) \end{array} \right]. \quad (3.4)$$

In the case of exponential decay, we have

$$\frac{1}{1-\alpha} \frac{s^\alpha \tilde{u}(s) - u(0)}{s + \frac{\alpha}{1-\alpha}} = \sum_{j=1}^n \left[\begin{array}{c} e^{-st_j} L(f_j(t+t_j, u(t+t_j))) \\ -e^{-st_{j-1}} L(f_{j-1}(t+t_{j-1}, u(t+t_{j-1}))) \end{array} \right]. \quad (3.5)$$

We present some simple examples:

$$\frac{dy(t)}{dt} = \begin{cases} t+1 & \text{if } t \in [0, T] \\ e^t + t & \text{if } t \in [T, T_1] \\ t^2 & \text{if } t > T_1 \end{cases}. \quad (3.6)$$

Thus, we write

$$\begin{aligned} \frac{dy(t)}{dt} &= (t+1)[u(t) - u(t-T)] + (e^t + t)[u(t-T) - u(t-T_1)] \\ &\quad + t^2 u(t-T_1). \end{aligned} \quad (3.7)$$

Applying the Laplace transform yields

$$\begin{aligned} s\tilde{u}(s) - u(0) &= L(t+1) - e^{-sT} L(t+T+1) + e^{-sT} L(e^{t+T} + t+T) \\ &\quad - e^{-sT_1} L(e^{t+T_1} + t+T_1) + e^{-sT_1} L((t+T_1)^2) \\ &= \frac{1}{s} + \frac{1}{s^2} - e^{-sT} \left(\frac{1}{s^2} + \frac{T+1}{s} \right) + e^{-sT} \left(\frac{e^T}{1+s} + \frac{1}{s^2} + \frac{T}{s} \right) \\ &\quad - e^{-sT_1} \left(\frac{e^{T_1}}{1+s} + \frac{1}{s^2} + \frac{T_1}{s} \right) + e^{-sT_1} \left(\frac{T_1^2}{s} + \frac{2T_1}{s^2} + \frac{2}{s^3} \right). \end{aligned} \quad (3.8)$$

Therefore, we can have

$$\begin{aligned} \tilde{u}(s) &= \frac{u(0)}{s} + \frac{1}{s^2} + \frac{1}{s^3} - e^{-sT} \left(\frac{1}{s^3} + \frac{T+1}{s^2} \right) + e^{-sT} \left(\frac{e^T}{s^2+s} + \frac{1}{s^3} + \frac{T}{s^2} \right) \\ &\quad - e^{-sT_1} \left(\frac{e^{T_1}}{s^2+s} + \frac{1}{s^3} + \frac{T_1}{s^2} \right) + e^{-sT_1} \left(\frac{T_1^2}{s^2} + \frac{2T_1}{s^3} + \frac{2}{s^4} \right). \end{aligned} \quad (3.9)$$

In the case of the power-law, one can obtain

$$\begin{aligned} \tilde{u}(s) &= \frac{u(0)}{s^{\alpha-1}} + \frac{1}{s^\alpha} + \frac{1}{s^{\alpha+1}} - e^{-sT} \left(\frac{1}{s^{\alpha+1}} + \frac{T+1}{s^\alpha} \right) + e^{-sT} \left(\frac{e^T}{s^\alpha + s^{\alpha-1}} + \frac{1}{s^{\alpha+1}} + \frac{T}{s^\alpha} \right) \\ &\quad - e^{-sT_1} \left(\frac{e^{T_1}}{s^\alpha + s^{\alpha-1}} + \frac{1}{s^{\alpha+1}} + \frac{T_1}{s^\alpha} \right) + e^{-sT_1} \left(\frac{T_1^2}{s^\alpha} + \frac{2T_1}{s^{\alpha+1}} + \frac{2}{s^{\alpha+2}} \right). \end{aligned} \quad (3.10)$$

For this example, we can now introduce the Bode diagram and phase diagram associated with this piecewise Laplace transform. In the case of the classical derivative, we consider $T = 3$ and $T_1 = 5$. The Bode diagram and phase diagram are presented in Figures 1 and 2 below.

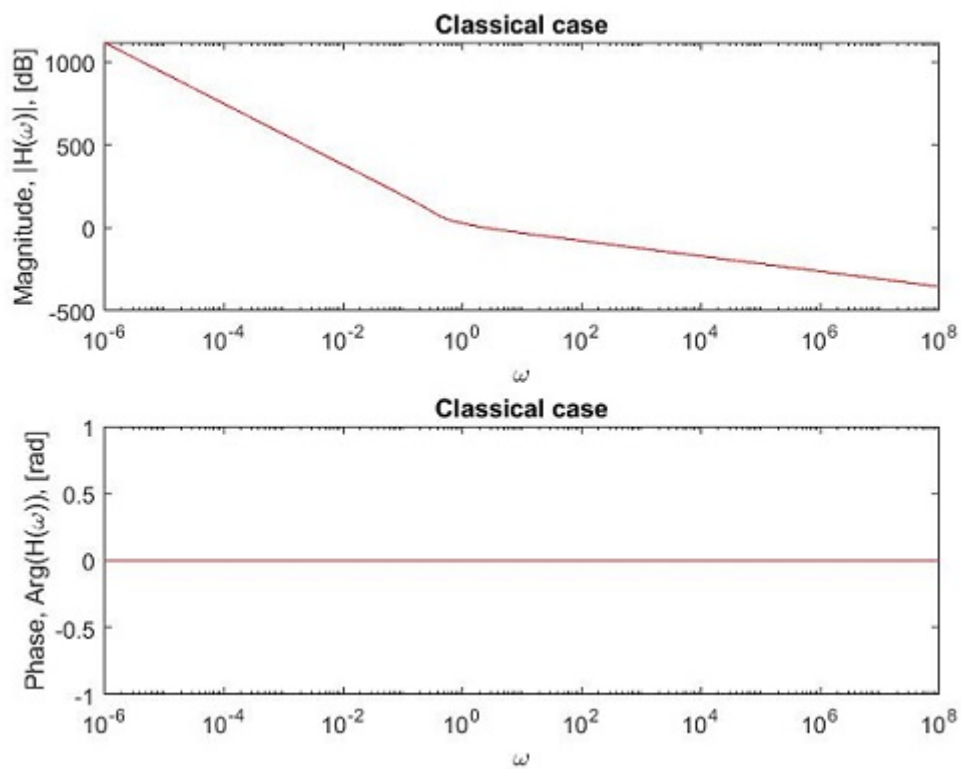


Figure 1. Bode and phase diagrams for the transfer function in Eq (3.9).

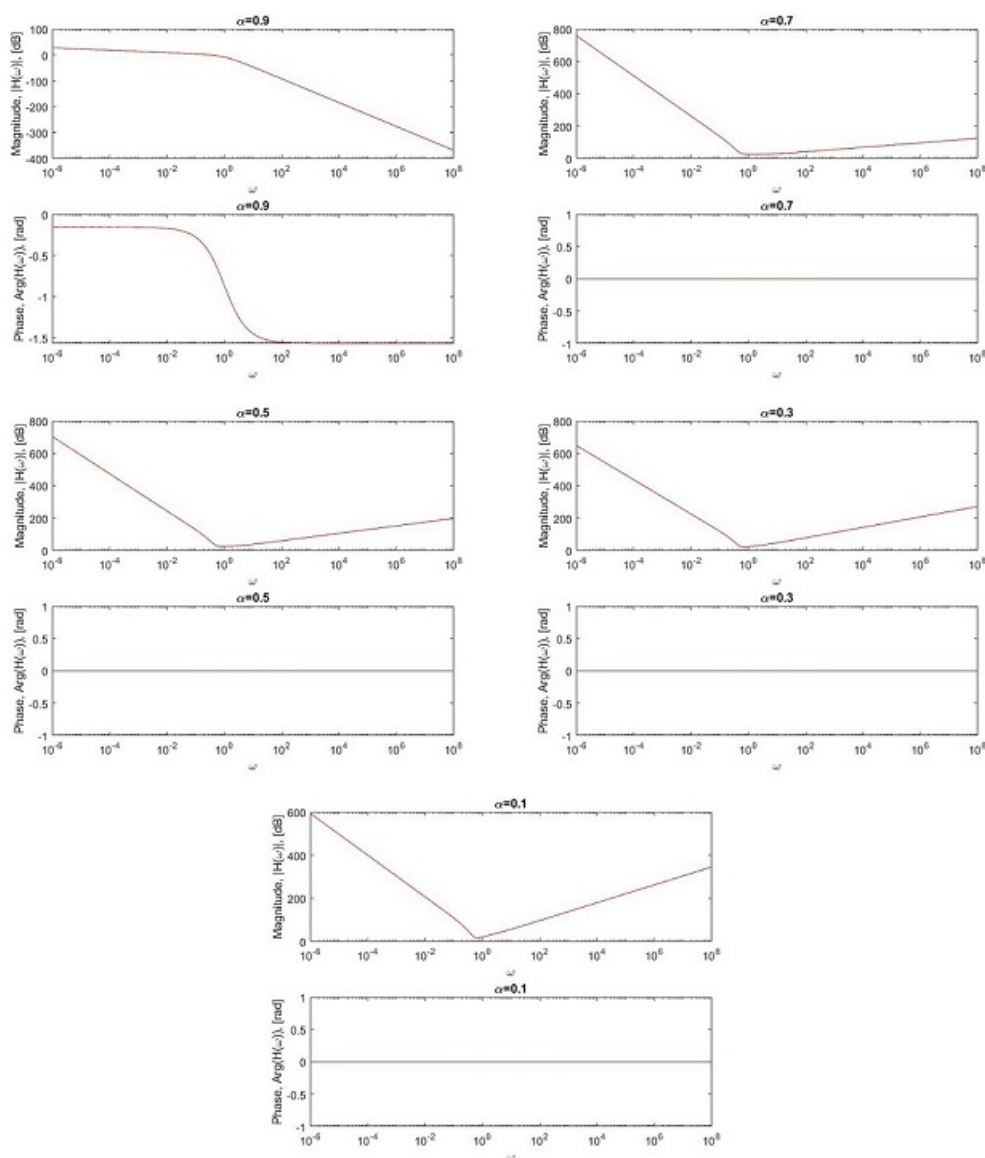


Figure 2. Bode and phase diagrams for the transfer function in Eq (3.10).

4. Some illustrative examples of piecewise differential equations

The translation of observable facts into mathematical models is one of the major limits of mathematical models. A good mathematical model should be thorough and contain practically all of the information found in the actual scenario. Some of these features were frequently left out of mathematical formulations by most mathematicians, and as a result, the conclusions of these models do not always match the data that have been seen, leading non-mathematicians to question the usefulness of mathematics. There is a need for a new class of ordinary and partial differential equations since differentiation, whether classical or piecewise, cannot capture these subtleties in its mathematical description. We give a few piecewise ordinary and partial differential equations in this section together

with their solutions and their graphical depictions.

$$\frac{dy}{dt} = \begin{cases} \begin{cases} 2 \cos t - 9y \cos t, & \text{if } t \in [0, 3], \\ y(0) = 0, \end{cases} \\ \begin{cases} \frac{1}{(2t^2+7)^2} - \frac{8ty}{2t^2+7}, & \text{if } t \in [3, 30] \end{cases} \end{cases} . \quad (4.1)$$

Using the Green's function technique yields

$$y(t) = \begin{cases} \begin{cases} \frac{2}{9} + c \exp(-9 \sin t), & \text{if } t \in [0, 3], \\ y(0) = 0, \end{cases} \\ \begin{cases} \frac{c+t}{2t^2+7}, & \text{if } t \in [3, 30], \\ y(3) = \frac{2}{9} - \frac{2}{9} \exp(-9 \sin 3) \end{cases} \end{cases} . \quad (4.2)$$

Applying the initial conditions, we obtain

$$y(t) = \begin{cases} \frac{2}{9} - \frac{2}{9} \exp(-9 \sin t), & \text{if } t \in [0, 3], \\ \frac{1}{2t^2+7} \left(\frac{23}{9} - \frac{50}{9} \exp(-9 \sin 3) + t \right), & \text{if } t \in [3, 5] \end{cases} . \quad (4.3)$$

In Figure 3, we present the solution of the above Cauchy problem. We present an example with the power-law

$${}^C D_t^\alpha y(t) = \begin{cases} -\lambda y(t), & \text{if } t \in [0, 1], \\ \exp(-\gamma t), & \text{if } t \in [1, t] \end{cases} . \quad (4.4)$$

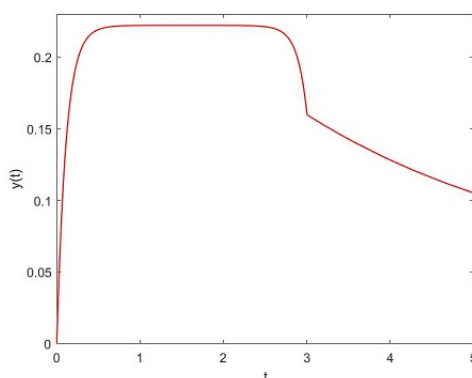


Figure 3. Solution of the piecewise Cauchy problem.

The solution is given as:

$$y(t) = \begin{cases} y(0) E_\alpha(-\lambda t^\alpha), & \text{if } t \in [0, 1], \\ y(0) + \frac{1}{\Gamma(\alpha)} \int_1^t e^{-\gamma \tau} (t - \tau)^{\alpha-1} d\tau, & \text{if } t \in [1, t] \end{cases} , \quad (4.5)$$

and

$$y(t) = \begin{cases} y(0) E_\alpha(-\lambda t^\alpha), & \text{if } t \in [0, 1], \\ \frac{1}{\Gamma(\alpha)} \sum_{j=1}^{\infty} \frac{(-\gamma)^j}{j!} \begin{bmatrix} t^{j+\alpha} B(j+1, \alpha) \\ -t^{j+\alpha} B\left(\frac{1}{t}, j+1, \alpha\right) \end{bmatrix}, & \text{if } t \in [1, t) \end{cases} \quad (4.6)$$

For $\gamma = 0$, we can consider the following problem:

$$y(t) = \begin{cases} y(0) E_\alpha(-\lambda t^\alpha), & \text{if } t \in [0, 1], \\ y(0) = 11, \\ y(1) + \frac{t^\alpha - 1}{\Gamma(\alpha+1)}, & \text{if } t \in [1, 10], \\ y(1) = y(0) E(-\lambda) \end{cases} \quad (4.7)$$

In Figure 4, we present the numerical simulation for the solution of the piecewise fractional differential equation where $\lambda = 1$ and $\gamma = 1$.

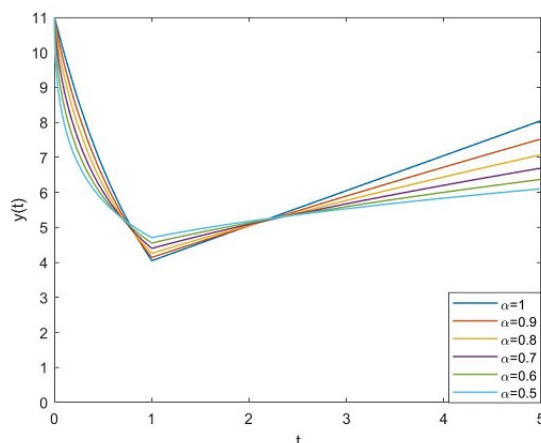


Figure 4. Solution of the piecewise Cauchy problem for different values of fractional order.

The findings shown in Figure 4 are quite fascinating and instructive since they show two different crossover tendencies. The idea of a piecewise differential equation whereby Mittag-Leffler decay is observed in the first portion and power-law growth is observed in the second induces the first crossover behaviors. In fact, this kind of crossover occurs frequently in real-world problems, even in ordinary human existence. The crossovers caused by the kernels are the second crossovers. After a crossover from stretched exponential to short memory power law decay in the first section, there are two crossings from short memory power law in the second portion. We now consider a piecewise partial differential equation where the first part is the heat equation and the second part is the advection-diffusion equation.

$$\frac{\partial}{\partial t} u(x, t) = \begin{cases} k \frac{\partial^2}{\partial x^2} u(x, t), & \text{if } t \in [0, 0.8], \\ \left\{ \frac{\partial^2}{\partial x^2} u(x, t) - a \frac{\partial}{\partial x} u(x, t) \right\}, & \text{if } t \in [0.8, 2], \end{cases} \quad (4.8)$$

where $k = 1$ and $a = 1$. The solution is obtained as

$$u(x, t) = \begin{cases} \begin{cases} 66 \sin \pi x \exp(-\pi^2 t), & \text{if } t \in [0, 0.8], \\ u(x, 0) = 66 \sin \pi x, u(0, t) = 0 \end{cases} \\ \begin{cases} 1/33 \exp(2t) (\exp(x) + \exp(-2x)), & \text{if } t \in [0.8, 2] \\ u(x, 0.8) = 1/33 e^{1.6} (\exp(x) + \exp(-2x)), \\ u(0.5, t) = 1/33 \exp(2t) (e^{0.5} + e^{-1}) \\ u(1, t) = 1/33 \exp(2t) (e + e^{-2}) \end{cases} \end{cases} \quad (4.9)$$

In Figure 5, the solution of the piecewise partial differential equation (4.9) is depicted.

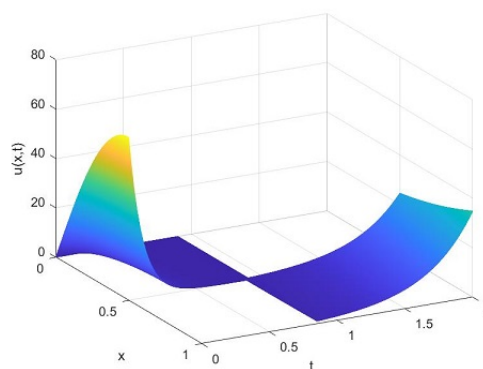


Figure 5. Solution of the piecewise partial differential equation (4.9).

4.1. Piecewise system: existence, uniqueness and numerical solution

If f_i is non-linear, the analytical methods may not be appropriate, while the numerical methods are suitable candidates to solve these problems. Nevertheless, to proceed with numerical analysis, it is worth proving that the piecewise ordinary differential equations admit unique solutions. One can find several approaches in the available literature; however, in this work, we only list the following. It is required that $\forall i \geq 1$, (f_i) satisfies the following conditions:

- 1) $|f_i(t, u(t))|^2 < k_i (1 + |u|^2)$, which is known as the growth condition,
- 2) $|f_i(t, u(t)) - f_i(t, v(t))|^2 < \tilde{k}_i |u - v|^2$, which is known as the Lipschitz condition.

Take

$$K = \max_{1 \leq i \leq n} |k_i| \quad \text{and} \quad \tilde{K} = \max_{1 \leq i \leq n} |\tilde{k}_i|. \quad (4.10)$$

Then, the equation admits a unique piecewise solution. The proof will not be presented here, as it can be found in several textbooks and published papers.

Having the conditions under which these equations admit exact piecewise solutions, owing to the fact that these equations are non-linear, there is no suitable analytical method that can be used to derive their exact solutions. In the following section, we shall derive their numerical solutions using the existing and modified numerical schemes. We shall start with a piecewise Cauchy problem in the

classical case,

$$\frac{d}{dt}u(t) = \begin{cases} f_1(t, u(t)) & \text{if } 0 \leq t \leq t_1 \\ \vdots & \\ f_n(t, u(t)) & \text{if } t_{k-1} \leq t \leq t_k \end{cases}. \quad (4.11)$$

Applying the classical integral on both sides leads to

$$u(t) = \begin{cases} u(0) + \int_0^t f_1(\tau, u(\tau)) d\tau, & \text{if } 0 \leq t \leq t_1 \\ \vdots & \\ u(t_{k-1}) + \int_{t_{k-1}}^t f_n(\tau, u(\tau)) d\tau & \text{if } t_{k-1} \leq t \leq t_k \end{cases}. \quad (4.12)$$

The integrand in the above equation can be approximated using the Adams-Bashforth approach to obtain

$$u(t_{k+1}) = \begin{cases} u(t_k) + \frac{h}{2} [3f_1(t_k, u(t_k)) - f_1(t_{k-1}, u(t_{k-1}))] \\ \vdots \\ u(t_k) + \frac{h}{2} [3f_n(t_k, u(t_k)) - f_n(t_{k-1}, u(t_{k-1}))] \end{cases}. \quad (4.13)$$

The same procedure can be repeated in the case of a piecewise non-linear ordinary differential equation with the Atangana-Baleanu fractional derivative, as presented below:

$${}_{0}^{ABC}D_t^\alpha u(t) = \begin{cases} f_1(t, u(t)) & \text{if } 0 \leq t \leq t_1 \\ \vdots & \\ f_n(t, u(t)) & \text{if } t_{k-1} \leq t \leq t_k \end{cases}. \quad (4.14)$$

We apply the Atangana-Baleanu integral on both sides to have

$$u(t) = \begin{cases} u(0) + (1 - \alpha) f_1(t, u(t)) + \frac{\alpha}{\Gamma(\alpha)} \int_0^t f_1(\tau, u(\tau)) (t - \tau)^{\alpha-1} d\tau, \\ \quad \text{if } 0 \leq t \leq t_1 \\ \vdots \\ u(t_{k-1}) + (1 - \alpha) f_n(t, u(t)) + \frac{\alpha}{\Gamma(\alpha)} \int_{t_{k-1}}^t f_n(\tau, u(\tau)) (t - \tau)^{\alpha-1} d\tau \\ \quad \text{if } t_{k-1} \leq t \leq t_k \end{cases}. \quad (4.15)$$

At this stage, several methods can be applied. For example, one can approximate these functions using polynomials. The following numerical scheme based on Newton polynomials [5] can be constructed

for the piecewise system with ABC derivative:

$$u(t_{k+1}) = \left\{ \begin{array}{l} \left\{ \begin{array}{l} u(0) + (1 - \alpha) f_1(t_k, u(t_k)) \\ + \left\{ \begin{array}{l} \frac{\alpha(\Delta t)^\alpha}{\Gamma(\alpha+1)} \sum_{m_1=2}^{l_1} f_1(t_{m_1-2}, u^{m_1-2}) \{(l_1 - m_1 + 1)^\alpha - (l_1 - m_1)^\alpha\} \\ + \frac{\alpha(\Delta t)^\alpha}{\Gamma(\alpha+2)} \sum_{m_1=2}^{l_1} [f_1(t_{m_1-1}, u^{m_1-1}) - f_1(t_{m_1-2}, u^{m_1-2})] \\ \times \left\{ \begin{array}{l} (l_1 - m_1 + 1)^\alpha (l_1 - m_1 + 3 + 2\alpha) \\ - (l_1 - m_1)^\alpha (l_1 - m_1 + 3 + 3\alpha) \end{array} \right\} \\ + \frac{\alpha(\Delta t)^\alpha}{2\Gamma(\alpha+3)} \sum_{m_1=2}^{l_1} \left[\begin{array}{l} f_1(t_{m_1}, u^{m_1}) - 2f_1(t_{m_1-1}, u^{m_1-1}) \\ + f_1(t_{m_1-2}, u^{m_1-2}) \end{array} \right] \end{array} \right\} \\ \times \left\{ \begin{array}{l} (l_1 - m_1 + 1)^\alpha \left[\begin{array}{l} 2(l_1 - m_1)^2 + (3\alpha + 10)(l_1 - m_1) \\ + 2\alpha^2 + 9\alpha + 12 \end{array} \right] \\ - (l_1 - m_1)^\alpha \left[\begin{array}{l} 2(l_1 - m_1)^2 + (5\alpha + 10)(l_1 - m_1) \\ + 6\alpha^2 + 18\alpha + 12 \end{array} \right] \end{array} \right\} \\ \text{if } 0 \leq t \leq t_1 \\ \vdots \\ u(t_{k-1}) + (1 - \alpha) f_n(t_k, u(t_k)) \\ + \left\{ \begin{array}{l} \frac{\alpha(\Delta t)^\alpha}{\Gamma(\alpha+1)} \sum_{m_k=l_{(k-1)+2}}^{l_k} f_1(t_{m_k-2}, u^{m_k-2}) \{(l_k - m_k + 1)^\alpha - (l_k - m_k)^\alpha\} \\ + \frac{\alpha(\Delta t)^\alpha}{\Gamma(\alpha+2)} \sum_{m_k=l_{(k-1)+2}}^{l_k} [f_1(t_{m_k-1}, u^{m_k-1}) - f_1(t_{m_k-2}, u^{m_k-2})] \\ \times \left\{ \begin{array}{l} (l_k - m_k + 1)^\alpha (l_k - m_k + 3 + 2\alpha) \\ - (l_k - m_k)^\alpha (l_k - m_k + 3 + 3\alpha) \end{array} \right\} \\ + \frac{\alpha(\Delta t)^\alpha}{2\Gamma(\alpha+3)} \sum_{m_k=l_{(k-1)+2}}^{l_k} \left[\begin{array}{l} f_1(t_{m_k}, u^{m_k}) - 2f_1(t_{m_k-1}, u^{m_k-1}) \\ + f_1(t_{m_k-2}, u^{m_k-2}) \end{array} \right] \\ \times \left\{ \begin{array}{l} (l_k - m_k + 1)^\alpha \left[\begin{array}{l} 2(l_k - m_k)^2 + (3\alpha + 10)(l_k - m_k) \\ + 2\alpha^2 + 9\alpha + 12 \end{array} \right] \\ - (l_k - m_k)^\alpha \left[\begin{array}{l} 2(l_k - m_k)^2 + (5\alpha + 10)(l_k - m_k) \\ + 6\alpha^2 + 18\alpha + 12 \end{array} \right] \end{array} \right\} \\ \text{if } t_{k-1} \leq t \leq t_k \end{array} \right. \end{array} \right. \quad (4.16)$$

Similarly, the same procedure is adopted when replacing the classical derivative with the Caputo-Fabrizio fractional derivative to obtain

$${}_0^{CF}D_t^\alpha u(t) = \begin{cases} f_1(t, u(t)) & \text{if } 0 \leq t \leq t_1 \\ \vdots & \\ f_n(t, u(t)) & \text{if } t_{k-1} \leq t \leq t_k \end{cases} \quad (4.17)$$

Thus, approximating the integrand using the well-known piecewise interpolation together with the parametrized concept [6], we obtain

$$u(t_{k+1}) = \begin{cases} \left[\begin{array}{l} u(t_k) + (1 - \alpha) (f_1(t_{k+1}, \tilde{u}_{k+1}) - f_1(t_k, u_k)) \\ + \alpha h \left\{ \left(1 - \frac{1}{2\rho}\right) f_1(t_k, u_k) + \frac{1}{2\rho} f_1(t_{k+1}, \tilde{u}_{k+1}) \right\} \end{array} \right], & \text{if } 0 \leq t \leq t_1 \\ \vdots & \\ \left[\begin{array}{l} u(t_k) + (1 - \alpha) (f_n(t_{k+1}, \tilde{u}_{k+1}) - f_n(t_k, u_k)) \\ + \alpha h \left\{ \left(1 - \frac{1}{2\rho}\right) f_n(t_k, u_k) + \frac{1}{2\rho} f_n(t_{k+1}, \tilde{u}_{k+1}) \right\} \end{array} \right], & \text{if } t_{k-1} \leq t \leq t_k \end{cases} \quad (4.18)$$

where

$$\tilde{u}_{k+1} = u_0 + (1 - \alpha) f_i(t_k, u_k) + \alpha h \sum_{j=0}^k f_i(t_j, u_j), i = 1, \dots, n. \quad (4.19)$$

Finally, we consider the following system with Caputo derivative:

$${}_0^C D_t^\alpha u(t) = \begin{cases} f_1(t, u(t)) & \text{if } 0 \leq t \leq t_1 \\ \vdots & \\ f_n(t, u(t)) & \text{if } t_{k-1} \leq t \leq t_k \end{cases}. \quad (4.20)$$

For this case, we derive the numerical solution using the Lagrange polynomial approach [7] to obtain

$$u(t_{k+1}) = \begin{cases} \left\{ u(0) + \begin{cases} \frac{(\Delta t)^\alpha}{\Gamma(\alpha+2)} \sum_{m_1=1}^{l_1} f_1(t_{m_1}, u^{m_1}) \begin{Bmatrix} (l_1 - m_1 + 1)^\alpha (l_1 - m_1 + 2 + \alpha) \\ -(l_1 - m_1)^\alpha (l_1 - m_1 + 2 + 2\alpha) \end{Bmatrix} \\ -\frac{(\Delta t)^\alpha}{\Gamma(\alpha+2)} \sum_{m_1=1}^{l_1} [f_1(t_{m_1-1}, u^{m_1-1})] \begin{Bmatrix} (l_1 - m_1 + 1)^\alpha \\ -(l_1 - m_1)^\alpha (l_1 - m_1 + 1 + \alpha) \end{Bmatrix} \end{cases} \right\} \\ \text{if } 0 \leq t \leq t_1 \\ \vdots \\ \left\{ u(t_{k-1}) + \begin{cases} \frac{(\Delta t)^\alpha}{\Gamma(\alpha+2)} \sum_{m_k=l_{(k-1)}+1}^{l_k} f_n(t_{m_k}, u^{m_k}) \begin{Bmatrix} (l_k - m_k + 1)^\alpha (l_k - m_k + 2 + \alpha) \\ -(l_k - m_k)^\alpha (l_k - m_k + 2 + 2\alpha) \end{Bmatrix} \\ -\frac{(\Delta t)^\alpha}{\Gamma(\alpha+2)} \sum_{m_k=l_{(k-1)}+1}^{l_k} f_n(t_{m_k-1}, u^{m_k-1}) \begin{Bmatrix} (l_k - m_k + 1)^\alpha \\ -(l_k - m_k)^\alpha (l_k - m_k + 1 + \alpha) \end{Bmatrix} \end{cases} \right\} \\ \text{if } t_{k-1} \leq t \leq t_k \end{cases}. \quad (4.21)$$

We provide numerous real-world examples, spanning from epidemiological modeling to chaos, in the next part to demonstrate the utility of the suggested notion in practice. However, it should be noted that this idea will be applied to a number of other real-world problems. To identify these crossover behaviors, a preliminary inquiry should be conducted.

5. Applications to mathematical biology

5.1. Tumor growth model: chemotherapy and radiotherapy

Every cancer kind calls for a different treatment plan, and thus, a precise cancer diagnosis is crucial for the right kind of treatment. Typically, systemic therapy, radiation and/or surgery are used in the treatment (chemotherapy, hormonal treatments, targeted biological therapies). The right choice of a treatment plan takes into account the patient as well as the malignancy. To obtain the anticipated therapeutic outcome, it is critical to complete the treatment procedure within the allotted period. Setting treatment objectives is a crucial first step. Typically, the main objective is to eradicate cancer or significantly extend life. A key objective is enhancing the patient's quality of life. Support for the patient's physical, emotional, and spiritual well-being as well as palliative care throughout the latter phases of cancer treatment might help achieve this. When discovered early and treated in accordance with best standards, some common cancer types, including breast cancer, cervical cancer, oral cancer and colorectal cancer, have high cure prospects. Even when malignant cells are present in other parts of the body, several cancer types, such as testicular seminoma and other forms of leukemia and lymphoma

in children, have excellent cure rates if adequate therapy is given. However, mathematical models have been used to assist in resolving these problems. Again, it remains very difficult to translate what is seen in a particular patient into a mathematical model. This may be because mathematicians do not fully comprehend biological processes or because biologists do not communicate with mathematicians using suitable mathematical words, which makes numerous mathematical models created for these circumstances less effective. We will discuss the potential use of the piecewise ordinary differential equations with a cancer model in this part.

Think about a woman who has breast cancer. Assume that surgery, chemotherapy, and radiation are also used in instances when cancer cells are more prone to spread throughout the body [8–10]. The piecewise system that models the two processes, in which chemotherapy is applied in the first process, and chemotherapy and radiotherapy are applied in the second process [9], is obtained as follows in order to model the change in cancer cells when these two treatment methods are used consecutively in the patient:

$$\left\{ \begin{array}{l} \frac{dT}{dt} = aT(1 - bT) - E_cCT \\ \frac{dE_c}{dt} = d_cE_c(1 - E_c) \\ \frac{dC}{dt} = -\gamma C \end{array} \right. \quad \text{if } 0 \leq t \leq t_1 \quad (5.1)$$

$$\left\{ \begin{array}{l} \frac{dT}{dt} = aT(1 - bT) - E_1(E_rDT + E_cCT) \\ \frac{dE_r}{dt} = d_rE_r(1 - E_r) \\ \frac{dE_c}{dt} = d_cE_c(1 - E_c) \\ \frac{dE_1}{dt} = d_1E_1(1 - E_1) \\ \frac{dC}{dt} = -\gamma C \end{array} \right. \quad \text{if } t_1 \leq t \leq \tilde{T}.$$

Here, the function T is the number of tumor cells, a is the tumor growth rate, and b is the reciprocal of the tumor carrying capacity. The function E_c describes the efficacy of the chemotherapy, the function C is the concentration of the chemotherapy, γ is the decay rate of the concentration, D is the amount of radiation, E_r is the efficacy of the radiotherapy, E_1 is the efficacy of the combined radiotherapy and chemotherapy, and the constants d_c , d_r and d_1 are the growth rates of the efficacy.

5.1.1. Numerical solution of the tumor growth model

The resultant model cannot be solved analytically due to its non-linearity; thus, a precise numerical method known as the predictor-corrector will be used and modified within the framework of the piecewise differential equations to solve the model. The graphical representation will be depicted in Figure 6.

$$\left\{ \begin{array}{l} \frac{dT}{dt} = aT(1 - bT) - E_cCT \\ \frac{dE_c}{dt} = d_cE_c(1 - E_c) \\ \frac{dC}{dt} = -\gamma C \end{array} \right. \quad \text{if } 0 \leq t \leq t_1 \quad (5.2)$$

$$\left\{ \begin{array}{l} \frac{dT}{dt} = aT(1 - bT) - E_1(E_rDT + E_cCT) \\ \frac{dE_r}{dt} = d_rE_r(1 - E_r) \\ \frac{dE_c}{dt} = d_cE_c(1 - E_c) \\ \frac{dE_1}{dt} = d_1E_1(1 - E_1) \\ \frac{dC}{dt} = -\gamma C \end{array} \right. \quad \text{if } t_1 \leq t \leq \tilde{T}.$$

We shall use some notations for simplicity:

$$\begin{aligned}
 X &= (T_j, E_{cj}, C_j), \\
 Y &= (T_j, E_{rj}, E_{cj}, E_j, C_j), \\
 F_i^* &= \begin{bmatrix} aT(1-bT) - E_cCT \\ d_cE_c(1-E_c) \\ -\gamma C \end{bmatrix}, \\
 G_m^* &= \begin{bmatrix} aT(1-bT) - E_1(E_rDT + E_cCT) \\ d_rE_r(1-E_r) \\ d_cE_c(1-E_c) \\ d_1E_1(1-E_1) \\ -\gamma C \end{bmatrix},
 \end{aligned} \tag{5.3}$$

such that $i = 1, \dots, 3, m = 1, \dots, 5$. The numerical solution of the above system is obtained as

$$\begin{cases} X(t_{k+1}) = X(t_k) + \frac{h}{2} \left[F_i^*(t_k, X_k) + F_i^*(t_{k+1}, X_{k+1}^p) \right], & 0 \leq t \leq t_1, \\ Y(t_{k+1}) = Y(t_k) + \frac{h}{2} \left[G_m^*(t_k, X_k) + G_m^*(t_{k+1}, Y_{k+1}^p) \right], & t_1 \leq t \leq \tilde{T} \end{cases}, \tag{5.4}$$

where

$$\begin{aligned}
 X^*(t_{k+1}, X_{k+1}^p) &= X(t_k) + hF_i^*(t_k, X_k), \\
 Y^*(t_{k+1}, Y_{k+1}^p) &= Y(t_k) + hG_m^*(t_k, Y_k).
 \end{aligned} \tag{5.5}$$

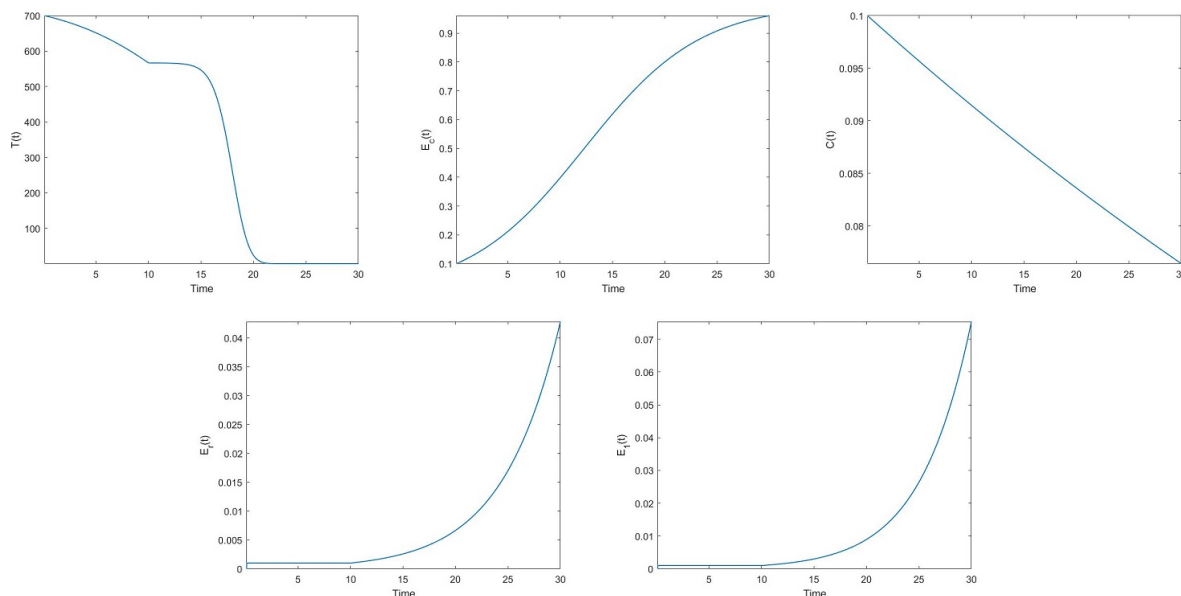


Figure 6. The numerical simulation for the tumor growth model.

In Figure 6, the numerical simulations are presented for the following initial data:

$$x(0) = 700, y(0) = 0.1, z(0) = 0.1, u(10) = 0, v(10) = 0, \quad (5.6)$$

and the parameters are chosen as

$$\begin{aligned} a &= 5 \times 10^{-11}, b = 0.0002, D = 100, d_c = 0.18, \\ d_r &= 0.19, d_1 = 0.22, \gamma = 0.009, t_1 = 10, T = 30. \end{aligned} \quad (5.7)$$

6. Applications to chaos

Nature is filled with chaos or exponential sensitivity to minor disturbances. Chaos is also expected to serve a variety of functional purposes in biological systems. Recently, with certain restrictions, methods for identifying chaos from empirical observations have developed. Such techniques need to be a crucial part of the biologist's repertoire. However, conventional algorithms for chaos identification are very sensitive to measurement noise and dissect typical edge situations, making it challenging to find chaos in fields like biology where data is noisy. Mathematical models are intended to simulate these observable phenomena. While some of these processes have been successfully replicated using current mathematical techniques, others still require proper modeling. The piecewise idea is used in this section to illustrate an expanded class.

6.1. Hybrid chaos: Arneodo and Bouali chaotic model

We consider a piecewise differential system where the first part is the Arneodo chaotic model that describes the dynamics of triple convection [12], and the second part is the Bouali chaotic system [11].

$$\left\{ \begin{array}{l} \frac{dx}{dt} = y \\ \frac{dy}{dt} = z \\ \frac{dz}{dt} = ax + by + cz - x^3. \end{array} \right. \quad \text{if } 0 \leq t \leq t_1 \quad (6.1)$$

$$\left\{ \begin{array}{l} \frac{dx}{dt} = a_1x(1-y) - \beta z \\ \frac{dy}{dt} = -b_1y(1-x^2) \\ \frac{dz}{dt} = \mu x \end{array} \right. \quad \text{if } t_1 \leq t \leq T$$

where initial conditions are taken as

$$x(0) = 1, y(0) = 1, z(0) = -0.02. \quad (6.2)$$

The parameters are chosen as

$$a = 0.8, b = -1.1, c = -0.45, a_1 = 0.003, \beta = 1.2, b_1 = 0.1, \mu = 0.7. \quad (6.3)$$

6.1.1. Numerical solution of the hybrid chaotic system

In this subsection, a hybrid chaotic model will be considered. In particular, we shall combine the Arneodo and Bouali models, the well-known chaotic models.

$$\left\{ \begin{array}{l} \frac{dx}{dt} = y \\ \frac{dy}{dt} = z \\ \frac{dz}{dt} = ax + by + cz - x^3 \end{array} \right. \quad \text{if } 0 \leq t \leq t_1 \quad (6.4)$$

$$x(0) = 0.1, y(0) = 0.1, z(0) = 0.1,$$

$$\left\{ \begin{array}{l} \frac{dx}{dt} = px(1-y) - \beta z \\ \frac{dy}{dt} = -by(1-x^2) \\ \frac{dz}{dt} = \mu x \end{array} \right. \quad \text{if } t_1 \leq t \leq T,$$

$$x(t_1) = 0.1, y(t_1) = 0.1, z(t_1) = 0.1.$$

The initial conditions are taken as

$$x(0) = 1, y(0) = 1, z(0) = -0.02. \quad (6.5)$$

The numerical simulations are depicted for the parameters $p = 0.003, \beta = 1.2, b = 0.1, \mu = 0.7, a = 0.8, c = -1.1, c = -0.45, t_1 = 1000$.

Using the Newton polynomial approach, the numerical solution of the Arneodo-Bouali chaotic system is obtained as:

$$x(t_{n+1}) = \left\{ \begin{array}{l} y^n + \sum_{k=2}^i \left\{ \begin{array}{l} \frac{5}{12}y^{k-2}\Delta t - \frac{4}{3}y^{k-1}\Delta t \\ + \frac{23}{12}y^k\Delta t \end{array} \right\}, \text{ if } 0 \leq t \leq t_1 \\ \left[x^1 + \sum_{k=i+2}^n \left\{ \begin{array}{l} \frac{5}{12}(a_1x^{k-2}(1-y^{k-2}) - \beta z^{k-2})\Delta t \\ - \frac{4}{3}(a_1x^{k-1}(1-y^{k-1}) - \beta z^{k-1})\Delta t \\ + \frac{23}{12}(a_1x^k(1-y^k) - \beta z^k)\Delta t \end{array} \right\} \right], \text{ if } t_1 \leq t \leq T \end{array} \right. , \quad (6.6)$$

$$y(t_{n+1}) = \left\{ \begin{array}{l} z^n + \frac{\alpha}{M(\alpha)} \sum_{k=2}^i \left\{ \begin{array}{l} \frac{5}{12}z^{k-2}\Delta t - \frac{4}{3}z^{k-1}\Delta t \\ + \frac{23}{12}z^k\Delta t \end{array} \right\}, \text{ if } 0 \leq t \leq t_1 \\ \left[y^1 + \sum_{k=i+2}^n \left\{ \begin{array}{l} \frac{5}{12}(-b_1y^{k-2}(1-x^{2k-4}))\Delta t \\ - \frac{4}{3}(-b_1y^{k-1}(1-x^{2k-2}))\Delta t \\ + \frac{23}{12}(-b_1y^k(1-x^{2k}))\Delta t \end{array} \right\} \right], \text{ if } t_1 \leq t \leq T \end{array} \right. , \quad (6.7)$$

$$z(t_{n+1}) = \left\{ \begin{array}{l} \left[\begin{array}{l} ax^n + by^n + cz^n - x^{3n} \\ + \sum_{k=2}^i \left\{ \begin{array}{l} \frac{5}{12}(ax^{k-2} + by^{k-2} + cz^{k-2} - x^{3k-6})\Delta t \\ - \frac{4}{3}(ax^{k-1} + by^{k-1} + cz^{k-1} - x^{3k-3})\Delta t \\ + \frac{23}{12}(ax^k + by^k + cz^k - x^{3k})\Delta t \end{array} \right\} \end{array} \right], \text{ if } 0 \leq t \leq t_1 \\ \left[z^1 + \sum_{k=i+2}^n \left\{ \begin{array}{l} \frac{5}{12}\mu x^{k-2}\Delta t - \frac{4}{3}\mu x^{k-1}\Delta t \\ + \frac{23}{12}\mu x^k\Delta t \end{array} \right\} \right], \text{ if } t_1 \leq t \leq T \end{array} \right. . \quad (6.8)$$

The numerical simulations for the above hybrid chaotic model are given in Figure 7.

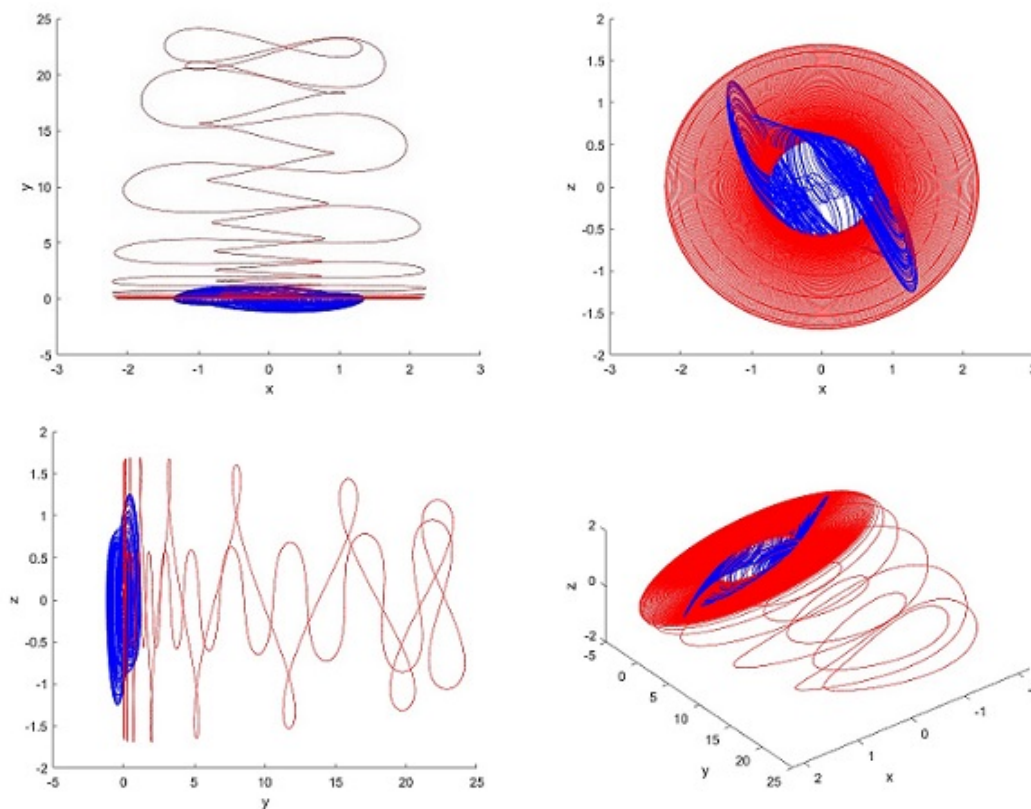


Figure 7. The numerical simulation for the Arneodo-Bouali chaotic system.

Replacing the first equation with the second one, the modified piecewise system called the Bouali-Arneodo chaotic model can be written as

$$\begin{cases} \frac{dx}{dt} = px(1-y) - \beta z \\ \frac{dy}{dt} = -b_1y(1-x^2) \\ \frac{dz}{dt} = \mu x \end{cases} \quad \text{if } 0 \leq t \leq t_1 \quad (6.9)$$

$$x(0) = 1, y(0) = 1, z(0) = -0.02,$$

$$\begin{cases} \frac{dx}{dt} = y \\ \frac{dy}{dt} = z \\ \frac{dz}{dt} = ax + by + cz - x^3. \end{cases} \quad \text{if } t_1 \leq t \leq T,$$

$$x(t_1) = 0.1, y(t_1) = 0.1, z(t_1) = 0.1.$$

In Figure 8, the numerical simulations are depicted for the parameters $p = 3, \beta = 2.2, b = -1.1, \mu = 0.001, a = 0.3, b_1 = 0.1, c = -0.45, t_1 = 800$.

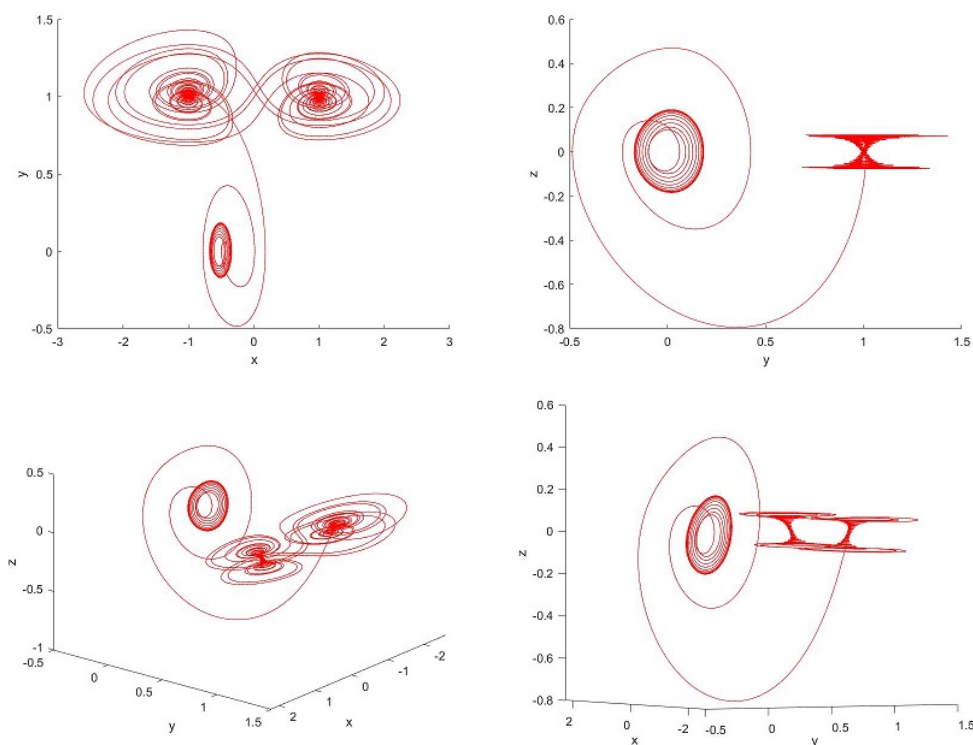


Figure 8. The numerical simulation for the Arneodo-Bouali chaotic system.

6.2. Hybrid chaos: King Cobra and Wang-Sun chaotic models

In this subsection, we shall consider the well-known King Cobra [13] and Wang-Sun [14] models to obtain a piecewise hybrid chaos model:

$$\begin{cases} \frac{dx}{dt} = a(y - x) + byz^2 \\ \frac{dy}{dt} = cx + dxz^2 \\ \frac{dz}{dt} = ez + fx \end{cases} \quad \text{if } 0 \leq t \leq t_1 \quad (6.10)$$

$$\begin{cases} \frac{dx}{dt} = a_1x + b_1yz \\ \frac{dy}{dt} = c_1x + d_1y - xz \\ \frac{dz}{dt} = e_1xy + f_1z \end{cases} \quad \text{if } t_1 \leq t \leq T.$$

The parameters are chosen as $a = 0.05, b = 1, c = 1, d = 0.5, e = -2, f = -1, a_1 = 0.2, b_1 = 1, c_1 = -7, d_1 = 0.0001, e_1 = 0.7, f_1 = 0.4$.

6.2.1. Numerical solution of the hybrid chaotic system

In this subsection, we deal with a hybrid chaotic system where King Cobra and Wang-Sun chaotic systems are considered.

$$\begin{cases} \frac{dx}{dt} = a(y-x) + byz^2 \\ \frac{dy}{dt} = cx + dxz^2 \\ \frac{dz}{dt} = ez + fx \end{cases} \quad \text{if } 0 \leq t \leq t_1 \quad (6.11)$$

$$x(0) = 0.1, y(0) = 0.1, z(0) = 0.1,$$

$$\begin{cases} \frac{dx}{dt} = a_1x + b_1yz \\ \frac{dy}{dt} = c_1x + d_1y - xz \\ \frac{dz}{dt} = e_1xy + f_1z \end{cases} \quad \text{if } t_1 \leq t \leq T,$$

$$x(t_1) = 0.1, y(t_1) = 0.1, z(t_1) = 0.1.$$

The associated numerical solution using the Newton polynomial is presented as:

$$x(t_{n+1}) = \begin{cases} \left(a(y^n - x^n) + by^n z^{2n} \right) \\ + \sum_{k=2}^i \left\{ \begin{array}{l} \frac{5}{12} (a(y^{k-2} - x^{k-2}) + by^{k-2} z^{2k-4}) \Delta t \\ -\frac{4}{3} (a(y^{k-1} - x^{k-1}) + by^{k-1} z^{2k-2}) \Delta t \\ +\frac{23}{12} (a(y^k - x^k) + by^k z^{2k}) \Delta t \end{array} \right\}, \text{ if } 0 \leq t \leq t_1 \\ \left[x^1 + \sum_{k=i+2}^n \left\{ \begin{array}{l} \frac{5}{12} (a_1 x^{k-2} + b_1 y^{k-2} z^{k-2}) \Delta t \\ -\frac{4}{3} (a_1 x^{k-1} + b_1 y^{k-1} z^{k-1}) \Delta t \\ +\frac{23}{12} (a_1 x^k + b_1 y^k z^k) \Delta t \end{array} \right\} \right], \text{ if } t_1 \leq t \leq T \end{cases}, \quad (6.12)$$

$$y(t_{n+1}) = \begin{cases} \left(cx^n + dx^n z^{2n} \right) \\ + \frac{\alpha}{M(\alpha)} \sum_{k=2}^i \left\{ \begin{array}{l} \frac{5}{12} (cx^{k-2} + dx^{k-2} z^{2k-4}) \Delta t \\ -\frac{4}{3} (cx^{k-1} + dx^{k-1} z^{2k-2}) \Delta t \\ +\frac{23}{12} (cx^k + dx^k z^{2k}) \Delta t \end{array} \right\}, \text{ if } 0 \leq t \leq t_1 \\ \left[y^1 + \sum_{k=i+2}^n \left\{ \begin{array}{l} \frac{5}{12} (c_1 x^{k-2} + d_1 y^{k-2} - x^{k-2} z^{k-2}) \Delta t \\ -\frac{4}{3} (c_1 x^{k-1} + d_1 y^{k-1} - x^{k-1} z^{k-1}) \Delta t \\ +\frac{23}{12} (c_1 x^k + d_1 y^k - x^k z^k) \Delta t \end{array} \right\} \right], \text{ if } t_1 \leq t \leq T \end{cases}, \quad (6.13)$$

$$z(t_{n+1}) = \begin{cases} \left(ez^n + fx^n \right) + \sum_{k=2}^i \left\{ \begin{array}{l} \frac{5}{12} (ez^{k-2} + fx^{k-2}) \Delta t \\ -\frac{4}{3} (ez^{k-1} + fx^{k-1}) \Delta t \\ +\frac{23}{12} (ez^k + fx^k) \Delta t \end{array} \right\}, \text{ if } 0 \leq t \leq t_1 \\ \left[z^1 + \sum_{k=i+2}^n \left\{ \begin{array}{l} \frac{5}{12} (e_1 x^{k-2} y^{k-2} + f_1 z^{k-2}) \Delta t \\ -\frac{4}{3} (e_1 x^{k-1} y^{k-1} + f_1 z^{k-1}) \Delta t \\ +\frac{23}{12} (e_1 x^k y^k + f_1 z^k) \Delta t \end{array} \right\} \right], \text{ if } t_1 \leq t \leq T \end{cases}. \quad (6.14)$$

In Figure 9, we depict the numerical simulations for the above hybrid chaotic model.

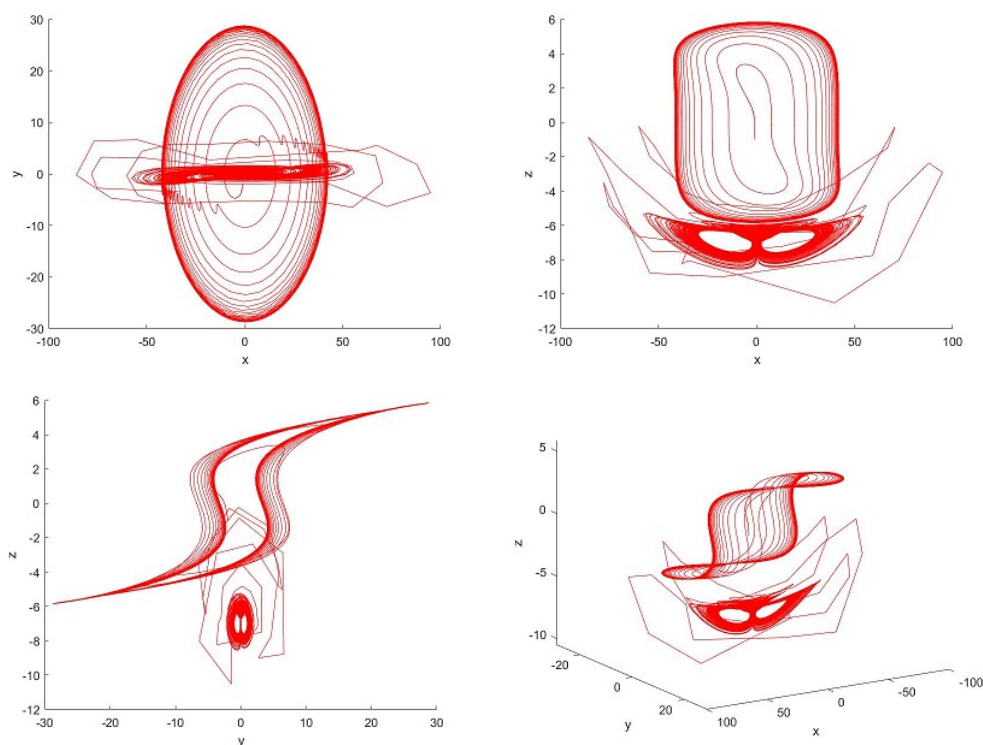


Figure 9. The numerical simulation for the King-Cobra-Wang-Sun chaotic system.

6.3. Hybrid chaos: Chen-Lee and Labyrinth chaotic models

In this subsection, the Chen-Lee system, which is based on the Euler equations for the motion of a rigid body [15], and the Labyrinth system, which describes the movement of a particle which moves in a labyrinth under the influence of some external source of energy [16], are represented by the following piecewise differential system:

$$\begin{cases} \frac{dx}{dt} = ax - yz \\ \frac{dy}{dt} = by + xz \\ \frac{dz}{dt} = cz + \frac{xy}{3} \end{cases} \text{ if } 0 \leq t \leq t_1, \quad (6.15)$$

$$\begin{cases} \frac{dx}{dt} = -\sin y(at) - bx(t) \\ \frac{dy}{dt} = -\sin z(at) - by(t) \\ \frac{dz}{dt} = -\sin x(at) - bz(t) \end{cases} \text{ if } t_1 \leq t \leq T,$$

where the initial conditions are taken as:

$$x(0) = 1, y(0) = 1, z(0) = -0.02. \quad (6.16)$$

The parameters are $a = 3, \beta = 2.2, b = 1, \mu = 0.001$.

6.3.1. Numerical solution of the hybrid chaotic system

In this subsection, we shall consider the well-known Chen-Lee [13] and Labyrinth [14] models to obtain a piecewise hybrid chaos model:

$$\begin{cases} \frac{dx}{dt} = ax - yz \\ \frac{dy}{dt} = by + xz \\ \frac{dz}{dt} = cz + \frac{xy}{3} \end{cases} \quad \text{if } 0 \leq t \leq t_1 \quad (6.17)$$

$$x(0) = 0.1, y(0) = 0.1, z(0) = 0.1,$$

$$\begin{cases} \frac{dx}{dt} = -\sin y(a_1t) - b_1x(t) \\ \frac{dy}{dt} = -\sin z(a_1t) - b_1y(t) \\ \frac{dz}{dt} = -\sin x(a_1t) - b_1z(t) \end{cases} \quad \text{if } t_1 \leq t \leq T,$$

$$x(t_1) = 0.1, y(t_1) = 0.1, z(t_1) = 0.1,$$

where the initial conditions are taken as:

$$x(0) = 1, y(0) = 1, z(0) = -0.02. \quad (6.18)$$

The parameters are taken as $p = 0.003, \beta = 1.2, b = 0.1, \mu = 0.7, a = 0.8, b = -1.1, c = -0.45, t_1 = 1000$.

Using the Newton polynomial approach, the numerical solution of the Chen-Lee-Labyrinth chaotic system is given by:

$$x(t_{n+1}) = \begin{cases} \left(ax^n - y^n z^n \right) + \sum_{k=2}^i \left\{ \begin{array}{l} \frac{5}{12} (ax^{k-2} - y^{k-2} z^{k-2}) \Delta t \\ -\frac{4}{3} (ax^{k-1} - y^{k-1} z^{k-1}) \Delta t \\ + \frac{23}{12} (ax^k - y^k z^k) \Delta t \end{array} \right\}, \text{ if } 0 \leq t \leq t_1 \\ \left[x^1 + \sum_{k=i+2}^n \left\{ \begin{array}{l} \frac{5}{12} (-\sin y(a_1 t_{k-2}) - b_1 x^{k-2}) \Delta t \\ -\frac{4}{3} (-\sin y(a_1 t_{k-1}) - b_1 x^{k-1}) \Delta t \\ + \frac{23}{12} (-\sin y(a_1 t_k) - b_1 x^k) \Delta t \end{array} \right\} \right], \text{ if } t_1 \leq t \leq T \end{cases}, \quad (6.19)$$

$$y(t_{n+1}) = \begin{cases} \left(bx^n + x^n z^n \right) + \frac{\alpha}{M(\alpha)} \sum_{k=2}^i \left\{ \begin{array}{l} \frac{5}{12} (bx^{k-2} + x^{k-2} z^{k-2}) \Delta t \\ -\frac{4}{3} (bx^{k-1} + x^{k-1} z^{k-1}) \Delta t \\ + \frac{23}{12} (bx^k + x^k z^k) \Delta t \end{array} \right\}, \text{ if } 0 \leq t \leq t_1 \\ \left[y^1 + \sum_{k=i+2}^n \left\{ \begin{array}{l} \frac{5}{12} (-\sin z(a_1 t_{k-2}) - b_1 y^{k-2}) \Delta t \\ -\frac{4}{3} (-\sin z(a_1 t_{k-1}) - b_1 y^{k-1}) \Delta t \\ + \frac{23}{12} (-\sin z(a_1 t_k) - b_1 y^k) \Delta t \end{array} \right\} \right], \text{ if } t_1 \leq t \leq T \end{cases}, \quad (6.20)$$

$$z(t_{n+1}) = \begin{cases} \left(cz^n + \frac{x^n y^n}{3} \right) + \sum_{k=2}^i \left\{ \begin{array}{l} \frac{5}{12} \left(cz^{k-2} + \frac{x^{k-2} y^{k-2}}{3} \right) \Delta t \\ -\frac{4}{3} \left(cz^{k-1} + \frac{x^{k-1} y^{k-1}}{3} \right) \Delta t \\ + \frac{23}{12} \left(cz^k + \frac{x^k y^k}{3} \right) \Delta t \end{array} \right\}, & \text{if } 0 \leq t \leq t_1 \\ \left[z^1 + \sum_{k=i+2}^n \left\{ \begin{array}{l} \frac{5}{12} \left(-\sin x (a_1 t_{k-2}) - b_1 z^{k-2} \right) \Delta t \\ -\frac{4}{3} \left(-\sin x (a_1 t_{k-1}) - b_1 z^{k-1} \right) \Delta t \\ + \frac{23}{12} \left(-\sin x (a_1 t_k) - b_1 z^k \right) \Delta t \end{array} \right\} \right], & \text{if } t_1 \leq t \leq T \end{cases} \quad (6.21)$$

In Figure 10, we depict the numerical simulations for the above hybrid chaotic model.

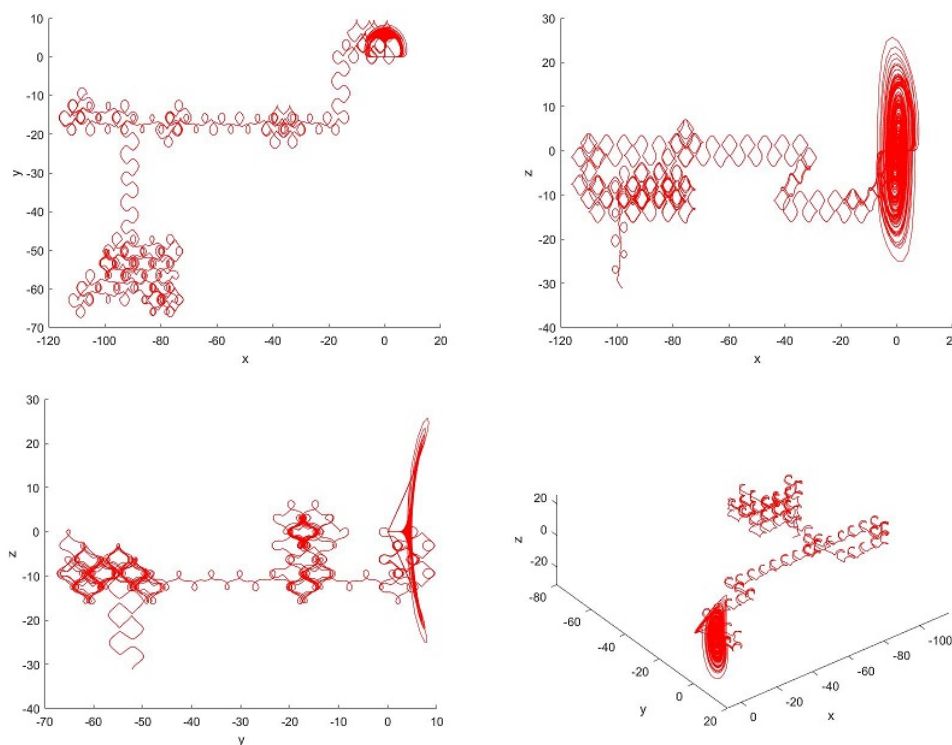


Figure 10. The numerical simulation for the Chen-Lee-Labyrinth chaotic system.

6.4. Hybrid chaos: Chen-Lee, Labyrinth and Dequan-Li chaotic models

In this subsection, we combine 3 well-known chaotic systems. The first part is the Chen-Lee system, the second part is the Labyrinth system and the last part is the Dequan-Li system, which is a three-dimensional quadratic autonomous chaotic system that displays an attractor with three scrolls [17].

$$\begin{cases} \frac{dx}{dt} = ax - yz \\ \frac{dy}{dt} = by + xz \\ \frac{dz}{dt} = cz + \frac{xy}{3} \end{cases} \quad \text{if } 0 \leq t \leq t_1 \quad (6.22)$$

$$x(0) = 0.1, y(0) = 0.1, z(0) = 0.1,$$

$$\begin{cases} \frac{dx}{dt} = -\sin y(a_1 t) - b_1 x(t) \\ \frac{dy}{dt} = -\sin z(a_1 t) - b_1 y(t) \quad \text{if } t_1 \leq t \leq t_2, \\ \frac{dz}{dt} = -\sin x(a_1 t) - b_1 z(t) \\ x(t_1) = 0.1, y(t_1) = 0.1, z(t_1) = 0.1, \\ \frac{dx}{dt} = a_2(y - x) + \delta xz \\ \frac{dy}{dt} = \rho x + \zeta y - xz \quad \text{if } t_2 \leq t \leq T \\ \frac{dz}{dt} = \gamma z + xy - \varepsilon x^2 \end{cases}$$

where the initial conditions are taken as:

$$x(0) = 1, y(0) = 1, z(0) = -0.02. \quad (6.23)$$

The parameters are considered as $p = 0.003, \beta = 1.2, b = 0.1, \mu = 0.7, a = 0.8, b = -1.1, c = -0.45, t_1 = 1000$.

6.4.1. Numerical solution of the hybrid chaotic system

In this subsection, we present the numerical solution of a piecewise chaotic system where Chen-Lee, Labyrinth and Dequan-Li chaotic systems are considered:

$$\begin{cases} \frac{dx}{dt} = ax - yz \\ \frac{dy}{dt} = by + xz \quad \text{if } 0 \leq t \leq t_1 \\ \frac{dz}{dt} = cz + \frac{xy}{3} \end{cases} \quad (6.24)$$

$$x(0) = 0.1, y(0) = 0.1, z(0) = 0.1,$$

$$\begin{cases} \frac{dx}{dt} = -\sin y(a_1 t) - b_1 x(t) \\ \frac{dy}{dt} = -\sin z(a_1 t) - b_1 y(t) \quad \text{if } t_1 \leq t \leq t_2, \\ \frac{dz}{dt} = -\sin x(a_1 t) - b_1 z(t) \\ x(t_1) = 0.1, y(t_1) = 0.1, z(t_1) = 0.1, \\ \frac{dx}{dt} = a_2(y - x) + \delta xz \\ \frac{dy}{dt} = \rho x + \zeta y - xz \quad \text{if } t_2 \leq t \leq T \\ \frac{dz}{dt} = \gamma z + xy - \varepsilon x^2 \end{cases}$$

where the initial conditions and parameters are chosen as

$$\begin{aligned} x(0) &= 1, y(0) = 1, z(0) = -0.02, p = 0.003, \beta = 1.2, b = 0.1, \\ \mu &= 0.7, a = 0.8, b = -1.1, c = -0.45, t_1 = 1000. \end{aligned} \quad (6.25)$$

Using the Newton polynomial approach, the numerical solution of the hybrid chaotic system is obtained as:

$$x(t_{n+1}) = \begin{cases} (ax^n - y^n z^n) \\ + \sum_{k=2}^{i_1} \left\{ \begin{array}{l} \frac{5}{12} (ax^{k-2} - y^{k-2} z^{k-2}) \Delta t \\ -\frac{4}{3} (ax^{k-1} - y^{k-1} z^{k-1}) \Delta t \\ + \frac{23}{12} (ax^k - y^k z^k) \Delta t \end{array} \right\}, \text{ if } 0 \leq t \leq t_1 \\ \left[x^1 + \sum_{k=i_1+2}^{i_2} \left\{ \begin{array}{l} \frac{5}{12} (-\sin y (a_1 t_{k-2}) - b_1 x^{k-2}) \Delta t \\ -\frac{4}{3} (-\sin y (a_1 t_{k-1}) - b_1 x^{k-1}) \Delta t \\ + \frac{23}{12} (-\sin y (a_1 t_k) - b_1 x^k) \Delta t \end{array} \right\} \right], \text{ if } t_1 \leq t \leq t_2, \\ \left[x^2 + \sum_{k=i_2+2}^n \left\{ \begin{array}{l} \frac{5}{12} (a_2 (y^{k-2} - x^{k-2}) + \delta x^{k-2} z^{k-2}) \Delta t \\ -\frac{4}{3} (a_2 (y^{k-1} - x^{k-1}) + \delta x^{k-1} z^{k-1}) \Delta t \\ + \frac{23}{12} (a_2 (y^k - x^k) + \delta x^k z^k) \Delta t \end{array} \right\} \right] \text{ if } t_2 \leq t \leq T, \end{cases} \quad (6.26)$$

$$y(t_{n+1}) = \begin{cases} (bx^n + x^n z^n) \\ + \frac{\alpha}{M(\alpha)} \sum_{k=2}^{i_1} \left\{ \begin{array}{l} \frac{5}{12} (bx^{k-2} + x^{k-2} z^{k-2}) \Delta t \\ -\frac{4}{3} (bx^{k-1} + x^{k-1} z^{k-1}) \Delta t \\ + \frac{23}{12} (bx^k + x^k z^k) \Delta t \end{array} \right\}, \text{ if } 0 \leq t \leq t_1 \\ \left[y^1 + \sum_{k=i_1+2}^{i_2} \left\{ \begin{array}{l} \frac{5}{12} (-\sin z (a_1 t_{k-2}) - b_1 y^{k-2}) \Delta t \\ -\frac{4}{3} (-\sin z (a_1 t_{k-1}) - b_1 y^{k-1}) \Delta t \\ + \frac{23}{12} (-\sin z (a_1 t_k) - b_1 y^k) \Delta t \end{array} \right\} \right], \text{ if } t_1 \leq t \leq t_2, \\ \left[y^2 + \sum_{k=i_2+2}^n \left\{ \begin{array}{l} \frac{5}{12} (\rho x^{k-2} + \zeta y^{k-2} - x^{k-2} z^{k-2}) \Delta t \\ -\frac{4}{3} (\rho x^{k-1} + \zeta y^{k-1} - x^{k-1} z^{k-1}) \Delta t \\ + \frac{23}{12} (\rho x^k + \zeta y^k - x^k z^k) \Delta t \end{array} \right\} \right] \text{ if } t_2 \leq t \leq T \end{cases} \quad (6.27)$$

$$z(t_{n+1}) = \begin{cases} (cz^n + \frac{x^n y^n}{3}) + \sum_{k=2}^{i_1} \left\{ \begin{array}{l} \frac{5}{12} (cz^{k-2} + \frac{x^{k-2} y^{k-2}}{3}) \Delta t \\ -\frac{4}{3} (cz^{k-1} + \frac{x^{k-1} y^{k-1}}{3}) \Delta t \\ + \frac{23}{12} (cz^k + \frac{x^k y^k}{3}) \Delta t \end{array} \right\}, \text{ if } 0 \leq t \leq t_1 \\ \left[z^1 + \sum_{k=i+3}^n \left\{ \begin{array}{l} \frac{5}{12} (-\sin x (a_1 t_{k-2}) - b_1 z^{k-2}) \Delta t \\ -\frac{4}{3} (-\sin x (a_1 t_{k-1}) - b_1 z^{k-1}) \Delta t \\ + \frac{23}{12} (-\sin x (a_1 t_k) - b_1 z^k) \Delta t \end{array} \right\} \right], \text{ if } t_1 \leq t \leq t_2, \\ \left[z^2 + \sum_{k=i+3}^n \left\{ \begin{array}{l} \frac{5}{12} (\gamma z^{k-2} + x^{k-2} y^{k-2} - \epsilon x^{2k-4}) \Delta t \\ -\frac{4}{3} (\gamma z^{k-1} + x^{k-1} y^{k-1} - \epsilon x^{2k-2}) \Delta t \\ + \frac{23}{12} (\gamma z^k + x^k y^k - \epsilon x^{2k}) \Delta t \end{array} \right\} \right] \text{ if } t_2 \leq t \leq T \end{cases} \quad (6.28)$$

In Figures 11 and 12, we present the numerical simulations for the above hybrid chaotic model.

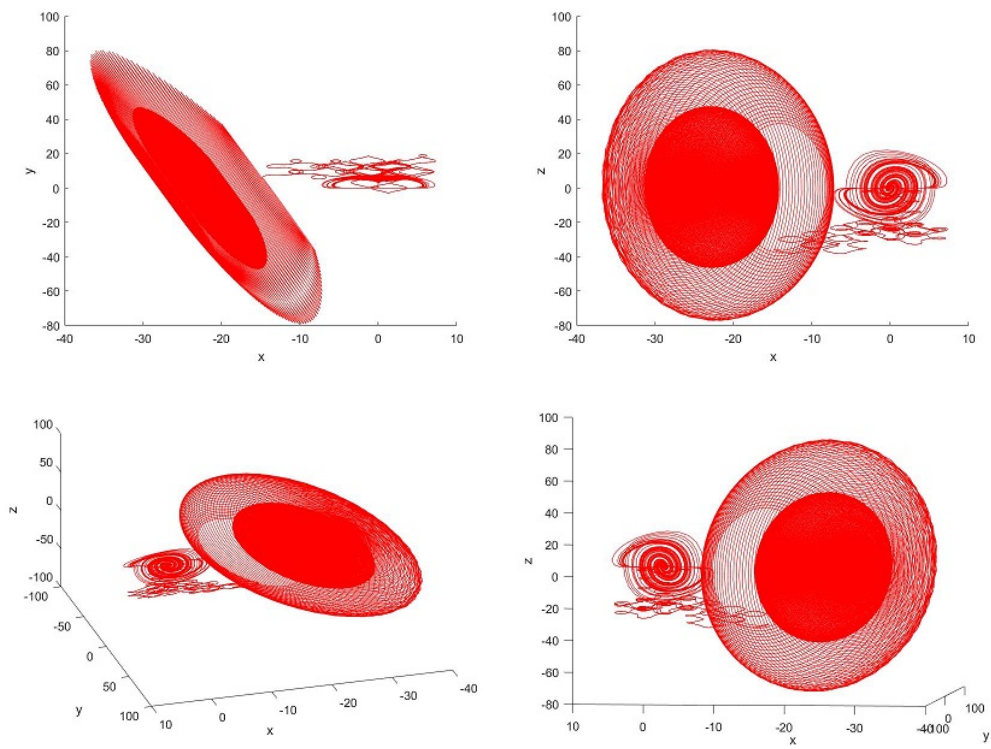


Figure 11. The numerical simulation for the Chen-Lee-Labyrinth-Dequan-Li chaotic system.

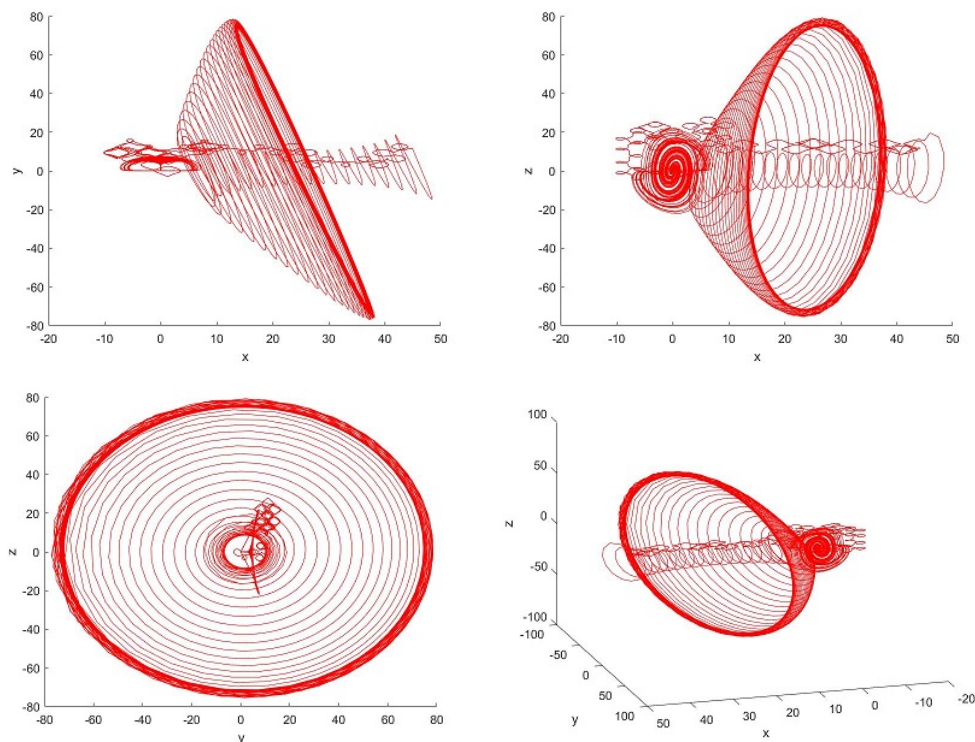


Figure 12. The numerical simulation for Chen-Lee-Labyrinth-Dequan-Li chaotic system.

6.5. Deterministic-Stochastic hybrid chaos: Bouali and Arneodo chaotic models

In this subsection, we shall consider the well-known Bouali and Arneodo models to obtain a piecewise hybrid chaos model:

$$\begin{cases} \begin{cases} \frac{dx}{dt} = ax(1-y) - \beta z \\ \frac{dy}{dt} = -by(1-x^2) \\ \frac{dz}{dt} = \mu x \end{cases} & \text{if } 0 \leq t \leq t_1 \end{cases} \quad (6.29)$$

$$\begin{cases} \begin{cases} dx = ydt + \sigma_1 x dB_1(t) \\ dy = zdt + \sigma_2 y dB_2(t) \\ dz = \left(\begin{matrix} ax + by \\ +cz - x^3 \end{matrix} \right) dt + \sigma_3 z dB_3(t). \end{cases} & \text{if } t_1 \leq t \leq T. \end{cases}$$

6.5.1. Numerical solution of the deterministic-stochastic hybrid chaotic system

In this subsection, we shall consider the well-known Bouali and Arneodo models to obtain a piecewise hybrid chaos model:

$$\begin{cases} \begin{cases} \frac{dx}{dt} = ax(1-y) - \beta z \\ \frac{dy}{dt} = -by(1-x^2) \\ \frac{dz}{dt} = \mu x \end{cases} & \text{if } 0 \leq t \leq t_1 \end{cases} \quad (6.30)$$

$$\begin{cases} dx = ydt + \sigma_1 x dB_1(t) \\ dy = zdt + \sigma_2 y dB_2(t) \\ dz = \begin{pmatrix} ax + by \\ +cz - x^3 \end{pmatrix} dt + \sigma_3 z dB_3(t). \end{cases} \quad \text{if } t_1 \leq t \leq T$$

where the initial conditions are chosen as

$$x(0) = 1, y(0) = 1, z(0) = -0.02. \quad (6.31)$$

The parameters are taken as $a = 3, \beta = 2.2, b = 1, \mu = 0.001$.

Using the Newton polynomial approach, the numerical solution of the deterministic stochastic chaotic system is obtained as:

$$x(t_{n+1}) = \begin{cases} \left[\begin{aligned} & (ax^n(1-y^n) - \beta z^n) \\ & + \sum_{k=2}^i \left\{ \begin{aligned} & \frac{5}{12} (ax^{k-2}(1-y^{k-2}) - \beta z^{k-2}) \Delta t \\ & - \frac{4}{3} (ax^{k-1}(1-y^{k-1}) - \beta z^{k-1}) \Delta t \\ & + \frac{23}{12} (ax^k(1-y^k) - \beta z^k) \Delta t \end{aligned} \right\} \end{aligned} \right], \text{ if } 0 \leq t \leq t_1 \\ \left[\begin{aligned} & x^1 + \sum_{k=i+2}^n \left\{ \begin{aligned} & \frac{5}{12} y^{k-2} \Delta t - \frac{4}{3} y^{k-1} \Delta t \\ & + \frac{23}{12} y^k \Delta t \end{aligned} \right\} \\ & + \sum_{k=i+2}^n \left\{ \begin{aligned} & \frac{5}{12} (B_1(t_{k-1}) - B_1(t_{k-2})) \sigma_1 x^{k-2} \\ & - \frac{4}{3} (B_1(t_k) - B_1(t_{k-1})) \sigma_1 x^{k-1} \\ & + \frac{23}{12} (B_1(t_{k+1}) - B_1(t_k)) \sigma_1 x^k \end{aligned} \right\} \end{aligned} \right], \text{ if } t_1 \leq t \leq T \end{cases}, \quad (6.32)$$

$$y(t_{n+1}) = \begin{cases} \left[\begin{aligned} & (-by^n(1-x^{2n})) \\ & + \frac{\alpha}{M(\alpha)} \sum_{k=2}^i \left\{ \begin{aligned} & \frac{5}{12} (-by^{k-2}(1-x^{2k-4})) \Delta t \\ & - \frac{4}{3} (-by^{k-1}(1-x^{2k-2})) \Delta t \\ & + \frac{23}{12} (-by^k(1-x^{2k})) \Delta t \end{aligned} \right\} \end{aligned} \right], \text{ if } 0 \leq t \leq t_1 \\ \left[\begin{aligned} & y^1 + \sum_{k=i+2}^n \left\{ \begin{aligned} & \frac{5}{12} z^{k-2} \Delta t - \frac{4}{3} z^{k-1} \Delta t \\ & + \frac{23}{12} z^k \Delta t \end{aligned} \right\} \\ & + \sum_{k=i+2}^n \left\{ \begin{aligned} & \frac{5}{12} (B_2(t_{k-1}) - B_2(t_{k-2})) \sigma_2 y^{k-2} \\ & - \frac{4}{3} (B_2(t_k) - B_2(t_{k-1})) \sigma_2 y^{k-1} \\ & + \frac{23}{12} (B_2(t_{k+1}) - B_2(t_k)) \sigma_2 y^k \end{aligned} \right\} \end{aligned} \right], \text{ if } t_1 \leq t \leq T \end{cases}, \quad (6.33)$$

$$z(t_{n+1}) = \begin{cases} \left[\begin{aligned} & \mu x^n + \sum_{k=2}^i \left\{ \begin{aligned} & \frac{5}{12} \mu x^{k-2} \Delta t - \frac{4}{3} \mu x^{k-1} \Delta t \\ & + \frac{23}{12} \mu x^k \Delta t \end{aligned} \right\} \end{aligned} \right], \text{ if } 0 \leq t \leq t_1 \\ \left[\begin{aligned} & z^1 + \sum_{k=i+2}^n \left\{ \begin{aligned} & \frac{5}{12} (ax^{k-2} + by^{k-2} + cz^{k-2} - x^{3k-6}) \Delta t \\ & - \frac{4}{3} (ax^{k-1} + by^{k-1} + cz^{k-1} - x^{3k-3}) \Delta t \\ & + \frac{23}{12} (ax^k + by^k + cz^k - x^{3k}) \Delta t \end{aligned} \right\} \\ & + \sum_{k=i+2}^n \left\{ \begin{aligned} & \frac{5}{12} (B_3(t_{k-1}) - B_3(t_{k-2})) \sigma_3 z^{k-2} \\ & - \frac{4}{3} (B_3(t_k) - B_3(t_{k-1})) \sigma_3 z^{k-1} \\ & + \frac{23}{12} (B_3(t_{k+1}) - B_3(t_k)) \sigma_3 z^k \end{aligned} \right\} \end{aligned} \right], \text{ if } t_1 \leq t \leq T \end{cases}. \quad (6.34)$$

In Figure 13, the numerical simulations are presented for the above hybrid chaotic model.

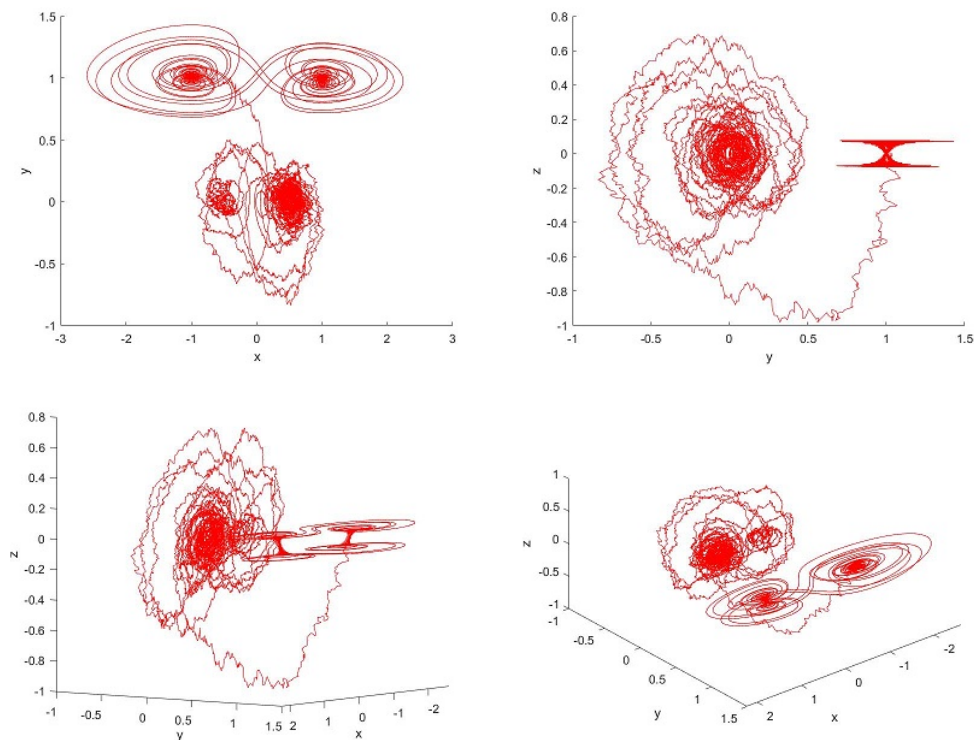


Figure 13. The numerical simulation of the deterministic Bouali and stochastic Arneodo system.

7. Conclusions

Although many processes in nature cannot be accurately duplicated using current conceptions, existing mathematical concepts have been applied to understand nature with considerable effectiveness. Therefore, researchers concentrate their efforts on developing new terminologies, frameworks, approaches and ideas that could be utilized to comprehend the complexity of nature. This is one of the main causes for the introduction of various differential operators and the accompanying integrals in recent decades, which have greatly enhanced modeling. On the other hand, mathematicians introduced the ideas of piecewise differential and integral operators and piecewise functions in response to changes that were noticed at various temporal or spatial scales. Although these two ideas, especially piecewise functions, have been theorized about, there are still processes in nature that existing models are unable to faithfully duplicate, despite the fact that these two notions, especially piecewise functions, have been employed in theory and applications to model processes with various patterns. In this work, we propose several piecewise differential equations and provide some significant conclusions ranging from theory to application. These results are based on the piecewise derivative and piecewise functions. Theoretical and practical avenues will be opened by this extension.

Conflict of interest

The authors declare that there is no conflict of interest.

References

1. A. Atangana, S. İğret Araz, New concept in calculus: piecewise differential and integral operators, *Chaos Soliton. Fract.*, **145** (2021), 110638. <https://doi.org/10.1016/j.chaos.2020.110638>
2. M. Caputo, Linear model of dissipation whose Q is almost frequency independent-II, *Geophys. J. Int.*, **13** (1967), 529–539. <https://doi.org/10.1111/j.1365-246X.1967.tb02303.x>
3. A. Atangana, D. Baleanu, New fractional derivatives with non-local and non-singular kernel: theory and application to heat transfer model, *Therm. Sci.*, **20** (2016), 763–769. <https://doi.org/10.2298/TSCI160111018A>
4. M. Caputo, M. Fabrizio, A new definition of fractional derivative without singular kernel, *Prog. Fract. Differ. Appl.*, **1** (2015), 73–85.
5. A. Atangana, S. İğret Araz, *New numerical scheme with Newton polynomial: theory, methods and applications*, Academic Press, 2021. <https://doi.org/10.1016/B978-0-12-775850-3.50017-0>
6. A. Atangana, S. İğret Araz, A modified parametrized method for ordinary differential equations with nonlocal operators, *HAL Science Ouverte*, **1** (2022), hal-03840759.
7. M. Toufik, A. Atangana, New numerical approximation of fractional derivative with non-local and non-singular kernel: application to chaotic models, *Eur. Phys. J. Plus*, **137** (2022), 191. <https://doi.org/10.1140/epjp/s13360-022-02380-9>
8. I. A. Arık, S. İğret Araz, Crossover behaviors via piecewise concept: a model of tumor growth and its response to radiotherapy, *Results Phys.*, **41** (2022), 105894. <https://doi.org/10.1016/j.rinp.2022.105894>
9. H. Hellal, H. Elabsy, H. Elkaranshawy, Mathematical model for combined radiotherapy and chemotherapy that fits with experimental data, *J. Phys. Conf. Ser.*, **2287** (2022), 012013. <https://doi.org/10.1088/1742-6596/2287/1/012013>
10. Z. Z. Qiu , Y. Y. Sun, X. He, J. Wei, R. Zhou, J. Bai, et al., Application of genetic algorithm combined with improved SEIR model in predicting the epidemic trend of COVID-19, *Sci. Rep.*, **12** (2022), 8910. <https://doi.org/10.1038/s41598-022-12958-z>
11. S. Bouali, A 3D strange attractor with a distinctive silhouette. The butterfly effect revisited, *24th ABCM International Congress of Mechanical Engineering*, 2013.
12. A. Arneodo, P. H. Couillet, E. A. Spiegel, The dynamics of triple convection, *Geophysical Astrophysical Fluid Dynamics*, **31** (1985), 1–48. <https://doi.org/10.1080/03091928508219264>
13. P. Muthukumar, P. Balasubramaniam, K. Ratnavelu, Synchronization and an application of a novel fractional order King-Cobra chaotic system, *Chaos*, **24** (2014), 033105. <https://doi.org/10.1063/1.4886355>
14. Z. H. Wang, Y. X. Sun, B. J. van Wyk, G. Y. Qi, M. A. van Wyk, A 3-D four-wing attractor and its analysis, *Braz. J. Phys.*, **39** (2009), 547–553. <https://doi.org/10.1590/S0103-97332009000500007>

15. H. K. Chen, C. I. Lee, Anti-control of chaos in rigid body motion, *Chaos Soliton. Fract.*, **21** (2004), 957–965. <https://doi.org/10.1016/J.CHAOS.2003.12.034>
16. R. Thomas, Deterministic chaos seen in terms of feedback circuits: analysis, synthesis, “labyrinth chaos”, *Int. J. Bifurcat. Chaos*, **9** (1999), 1889–1905. <https://doi.org/10.1142/S0218127499001383>
17. D. Q. Li, A three-scroll chaotic attractor, *Phys. Lett. A*, **372** (2008), 387–393. <https://doi.org/10.1016/j.physleta.2007.07.045>
18. M. Alqhtani, K. M. Owolabi, K. M. Saad, E. Pindza, Spatiotemporal chaos in spatially extended fractional dynamical systems, *Commun. Nonlinear Sci.*, **119** (2023), 107118. <https://doi.org/10.1016/j.cnsns.2023.107118>
19. K. M. Owolabi, K. C. Patidar, A. Shikongo, A fitted operator method for a system of delay model of tumor cells dynamics within their micro-environment, *Appl. Math. Inform. Sci.*, **16** (2022), 367–388. <https://doi.org/10.18576/amis/160225>



AIMS Press

©2023 the Author(s), licensee AIMS Press. This is an open access article distributed under the terms of the Creative Commons Attribution License (<http://creativecommons.org/licenses/by/4.0>)